Examination of Kinect's Torso PCA Model for Planar Activities Assessment after Stroke

P N. Nordin, S.Q. Xie, B. Wuensche

Abstract*— Compensatory movement after stroke occurred when inter-joint coordination between arm and forearm for the purpose of arm transport becomes limited due to the weaknesses of the upper limb after stroke. This limitation causes an inefficiency of hand movement to perform the activity of daily living (ADL). Previous work has shown the possibility of using Kinect to assess torso compensation in typical assessment of upper limb movement in a stroke-simulated setting using a Torso Principal Component Analysis (PCA) Model. This research extends the study into evaluating Torso PCA Model in terms of orientation angles of the torso in three dimensional when performing planar activities namely circle tracing and point-to-point tracing. The orientation angles were compared to the outcome of the measurement from a standard motion capture system and Kinect's intrinsic chest orientation angles. Based on the statistical results, Torso PCA model is concurrently valid with the clinically accepted measures of torso orientation and can be used further to analyze torso compensation in stroke patients.

Keywords: Compensatory movement, PCA, stroke, torso angle.

I. INTRODUCTION

In healthy individuals, the redundancies in the upper limb joints enable the production of different strategies to complete the activities of daily living (ADL) such as brushing, eating and drinking [1]. However, severely affected stroke patients are more likely to impose couplings of joints to complete the task than healthy subjects due to pathologically limited arm-forearm coordination [2].

In the lack of distal voluntary movement, stroke patients frequently integrate the use of compensatory strategies to help arm transport to accomplish better functions and positioning. The existence of compensatory movement may suggest that the patient has not achieved a natural neurological recovery and that the patient has obtained a pattern of learned non-use during the voluntary movement evaluation. In [3] defines motor compensation as the appearance of new motor patterns resulting from the adaptation of remaining motor elements or substitution. They suggested that the compensation include the use of movement patterns that incorporate trunk displacement and rotation, scapular elevation, shoulder abduction, and internal rotation [4].

In [5] used the ratio of sagittal displacement between the index marker and the sternal marker to the sagittal displacement of the sternal marker as measures of arm-trunk compensation in the bimanual and unimanual study against healthy controls. The unimanual group recorded more pronounced trunk compensation while the bimanual group resulted in more significant improvements in the reduction of compensatory trunk movements in targeted reaching activity.

Previous work has shown that Torso PCA model is useful to represent compensatory movement after stroke [6]. This model is developed by harnessing Kinect's waist, spine, chest, collar, and shoulder positions in three dimensional. Then, they were used to compute a 3D orthonormal basis using PCA, thus representing a torso coordinate system.

Using Torso PCA model, the compensatory strategies can be observed. For example, when recording the movement of a patient with no pathological disorder who sits upright and tries to drink from a cup as shown in Fig. 1. In a typical normal behavior, her torso remains relatively stable. Hence, body joints associated with the torso will remain at similar locations in space throughout the recording and thus would produce similar variations. Stroke patient, however, would try to compensate the weaker arm using her upper body to reach for the cup. This compensatory movement would create a more considerable variation of torso principal components vectors during recording.

Compensatory assessment in stroke rehabilitation is able to highlight the patient's progress and, in particular, the contribution made by the intervention to improving the impairment of the patient. Reaching task is usually selected because it is the fundamental component in many daily activities, needs inter-joint coordination and extensively studied to understand upper limb movements [7]. In motion capture settings, quantitative measures in reaching, reach and grasp as well as drawing trajectories show significant results in delineating the degradation of movement quality after stroke in comparison to a healthy person [8].

Therefore, this study attempts to evaluate Kinect's Torso PCA model using motion capture as one of the measures of torso movement to highlight the lack of efficiency in stroke patients to complete planar activities assessment through motor compensation.

II MATERIAL AND METHODS

Ten male participants with no known history of upper limb impairments (mean age, 26.8 ± 5.6 years) participated in this study. All participants gave their informed consent to the study, which had been previously approved by the University of Auckland Human Participants Ethics Committee (UAHPEC).

Revised Manuscript Received on September 14, 2019.

N. Nordin, Center of Robotics and Industrial Automation, Universiti Teknikal Malaysia Melaka, Melaka, Malaysia. (Email: nurdiana@utem.edu.my)

S.Q. Xie, School of Electronic and Electrical Engineering, University of Leeds, Leeds, UK.

B. Wuensche, Department of Computer Science, University of Auckland, Auckland, New Zealand..

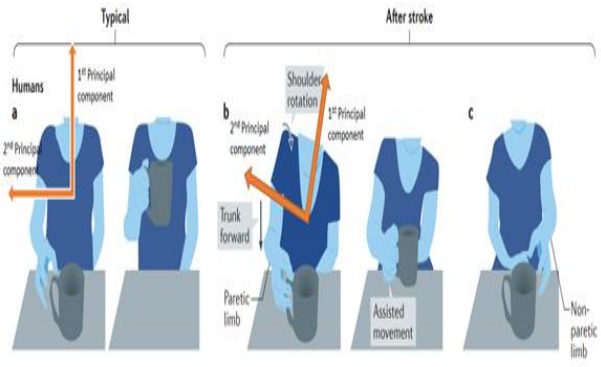

Fig. 1.Illustration of compensated movement during reaching. When not instructed to use the affected arm (paretic limb), patient often assist the movement with non-affected arm (non-paretic limb) [9].

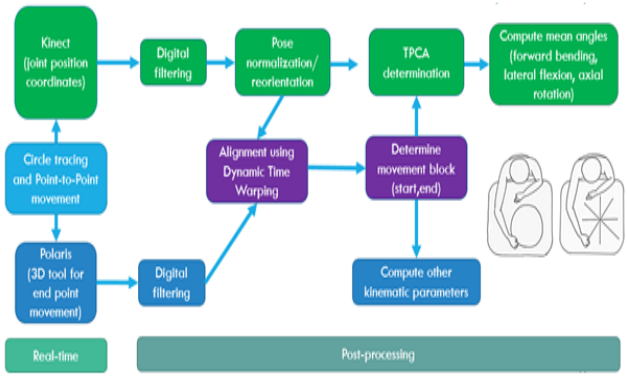

Fig. 2.An overall workflow of how data is collected and computed for Kinect's joint prediction validation against marker-based model

All participants were informed of the study requirements and agreed to participate in the tests. Participants were instructed to remove their clothing from the upper and were seated on an adjustable stool located 2.5 m in front of the Kinect v2. Kinect v2 will then track joint coordinates of the subject's body producing a skeletal outline, which was used as the reference for its measurements. The participants were also positioned in the middle of the 12-camera 3D motion analysis system (VICON, 12 MXT40s cameras, Vicon Nexus software, frequency: 100 Hz).

A total of 40 spherical markers (radius = 8 mm) were attached to bone landmarks on the subject's upper body in which 4 of them were directly used for the clinical definition of torso movements. The sampling rate of Kinect v2 and the 3D motion analysis system was 30 Hz and 100 Hz, respectively. Data post-processing for both systems was performed using MATLAB (MATLAB R2015a; MathWorks, Natick, MA, USA). The overall workflow is depicted in Fig. 2.

In this research, Kinect V2 and VICON data were not synchronized in real-time. Instead, a Dynamic Time-Warping procedure was computed to determine the frame difference. Firstly, the VICON data is down-sampled to Kinect's sampling rate (30Hz). This method was chosen to limit uncertainty of Kinect's prediction on unknown time points when it is up-sampled to VICON's sampling rate (100Hz).

The start and end points of VICON recording and Kinect's recording vary across data. Hence, we chose to use a dynamic time warping technique which outputs the frame difference of the hand and elbow position from both recordings to reconcile the difference.

The participants were instructed to perform two planar tracing task namely point to-point task (PTP) and circle drawing task (CT) using a 3D tool as depicted in Fig. 3. The endpoint of the tip is considered as the hand tracing data. This data became the basis for several computations of movement quality parameters such as temporal efficiency, spatial efficiency, movement duration, ease and smoothness.

Three instruments for measuring torso movement were compared: The Torso PCA (TPCA) model using Kinect v2's joint data, Kinect's readily available chest orientation angles and the ISB marker model using marker-based 3D motion analysis system.

Each participant was instructed to perform dynamic movements of tracing planar drawings (circle and center-out point-to-point drawing). The subjects were asked to determine randomly where the end-position of the hand for each task to reduce the bias of repeated measurements. Torso movements are measured based on its position and orientation in space.

Fig. 3.The 3D tool used to draw the circle and perform PTP task.

III. TORSO ANGLE MEASUREMENTS

Rotations are described using Euler angles. Thoracic movement is defined relative to the global coordinate system by defining both the coordinate systems according to the marker-based location as tabulated in Table I and depicted in Fig. 4. The thorax coordinate system and the global coordinate system are represented by the orthonormal basis tuple $\{\mathbf{X_T}, \mathbf{Y_T}, \mathbf{Z_T}\}$ and $\{\mathbf{X_G}, \mathbf{Y_G}, \mathbf{Z_G}\}$ respectively. To define the torso coordinate system, four marker locations are required to locate the anatomical landmarks. They are Incisura Jugularis (IJ), Processus Xiphoideus (PX), Processus Spinosus of the 8th thoracic vertebra (T8) and Processus Spinosus of the 7th cervical vertebra (C7). The global coordinate system is chosen arbitrarily.

According to ISB [10], whenever the global coordinate system and thorax joint coordinate system are defined this way, the rotation of the thorax with respect to the global coordinate system can be distinguished by three subsequent rotation following the Euler Z-X-Y rotation. Table II explains the clinical definition of torso movements relative to the global coordinate system when measured using a marker-based motion capture system.

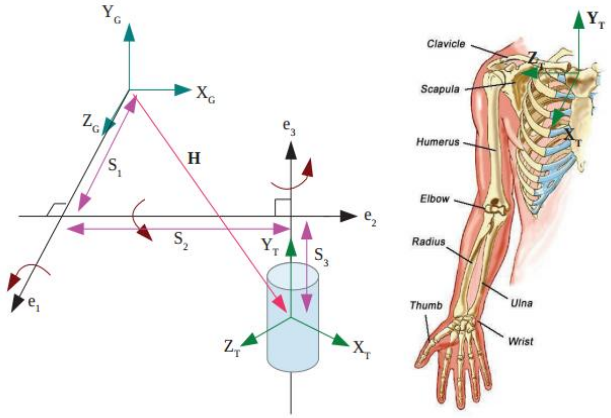

Fig. 4.Torso coordinate system relative to global coordinate system.

The suggested interpretation of the torso movements is by using Grood and Suntay method of floating axes. This method requires the characterization of proximal coordinate system {**I,J,K**} and distal coordinate system {**i,j,k**} to define the axes. The thorax coordinate system is therefore defined as distal coordinate system and the global coordinate system is the proximal coordinate system. These floating axes are non-orthonormal axes {$\mathbf{e_1}$, $\mathbf{e_2}$, $\mathbf{e_3}$} and are chosen to avoid gyroscopic singularities. The first rotation is around the body-fixed axis of the proximal coordinate system ($\mathbf{e_1}$) and the last rotation is around the body-fixed longitudinal axis of the moving segment ($\mathbf{e_3}$).

Table- I: Torso segment coordinate system

Segment Coordinate System	**Definition**
Origin	Co-incident with Incisura Jugularis (IJ)
X-axis ($\mathbf{X_T}$)	The common line perpendicular to the Z and Y axis pointing forward
Y-axis ($\mathbf{Y_T}$)	The line connecting midpoint between Processus Xiphoideus (PX) and Processus Spinosus of the 8th thoracic vertebra (T8); and the midpoint between IJ and Processus Spinosus of the 7th cervical vertebra (C7), pointing upward
Z-axis ($\mathbf{Z_T}$)	The line perpendicular to the plane formed by IJ, C7; and the midpoint between PX and T8, pointing to the right

Table- II: Clinical definition of torso movement

Movement	**Definition**
Translation	The displacement of marker position at Incisura Jugularis (IJ) of the participant
Flexion (negative)/ Extension (positive)	The angle between global y-axis with the intermediate rotation vector (the floating axis) in which the 3D rotation is resolved through Euler Z-X-Y convention
Axial rotation left (positive)/ right (negative)	The angle between x-axis of the thorax coordinate system with the intermediate rotation vector (the floating axis)
Lateral flexion right (negative)/ left (positive)	The angle between z-axis of the global coordinate system with the y-axis of the thorax coordinate system

The second axis, by definition, is perpendicular to both first and third rotation axes ($\mathbf{e_2}$). According to this definition, the first rotation is around $\mathbf{Z_G}$ of the global coordinate system and the last rotation is around $\mathbf{Y_T}$ of the thorax coordinate system. The detailed axes definition is tabulated in Table III.

Using this torso axes assignment, the flexion/extension angle (α), axial rotation angle (γ) and lateral flexion angle (β) are therefore defined as stated in (1) - (3) respectively.

$$e_1^r . e_2 = \cos\alpha \tag{1}$$

$$e_3^r . e_2 = \cos\gamma \tag{2}$$

$$e_1 . e_3 = \cos\beta \tag{3}$$

Table- III: Torso axes assignment according to Grood and Suntay method of floating axes

Axis	**Definition**
$\mathbf{e_1}$ (body fixed)	**K** (around $\mathbf{Z_G}$)
$\mathbf{e_3}$ (body fixed)	**j** (around $\mathbf{Y_T}$)
$\mathbf{e_1^r}$ (reference)	**J** (perpendicular to $\mathbf{e_1}$ about $\mathbf{Y_G}$ axis)
$\mathbf{e_3^r}$ (reference)	**i** (perpendicular to $\mathbf{e_3}$ about $\mathbf{X_T}$ axis)

To enable the computation of flexion/extension, axial rotation and lateral flexion angles respectively, the relative movement of the torso relative to the global coordinate system must be determined by firstly computing the direction cosine matrix (DCM) as stated in (4):

$$[R]^T = \begin{bmatrix} I.i & J.i & K.i \\ I.j & J.j & K.j \\ I.k & J.k & K.k \end{bmatrix} \tag{4}$$

This direction cosine matrix is also identical to the rotation matrix, **R** through a transpose, which explains the use of the previous DCM convention, $[R]^T$. The component of this matrix is numerically found by computing the dot product between the proximal and the distal axis. By equating the DCM to the Euler Z-X-Y rotation matrix, the DCM can now be interpreted as stated in (5).

$$[R]^T = \begin{bmatrix} -\sin\alpha\cos\gamma - \cos\alpha\cos\beta\sin\gamma & \cos\alpha\cos\gamma - \sin\alpha\cos\beta\sin\gamma & \sin\beta\sin\gamma \\ -\cos\alpha\sin\beta & -\sin\alpha\sin\beta & \cos\beta \\ \sin\gamma\sin\alpha - \cos\alpha\cos\beta\cos\gamma & -\cos\alpha\sin\gamma - \sin\alpha\cos & \sin\beta\cos\gamma \end{bmatrix} \tag{5}$$

The flexion/extension angle (α), axial rotation angle (γ) and lateral flexion angle (β) can thus be found as presented in (6) – (8).

$$\alpha = \tan^{-1}\left(\frac{-\sin\alpha\sin\beta}{-\cos\alpha\sin\beta}\right) = \tan^{-1}\left(\frac{J.j}{I.j}\right) \quad (6)$$

$$\gamma = \tan^{-1}\left(\frac{\sin\beta\sin\gamma}{\sin\beta\cos\gamma}\right) = \tan^{-1}\left(\frac{K.i}{K.k}\right) \quad (7)$$

$$\beta = \cos^{-1}(\cos\beta) = \cos^{-1}(K.j) \quad (8)$$

These clinical definitions of torso orientation angles are used as benchmark to evaluate torso angle measurements obtained from Torso PCA model using Kinect [6]. Principal component analysis was performed to the seven joints in Kinect's skeleton data provided by Brekel Probody v2 software [11] namely waist, spine, chest, left and right collar as well as left and right shoulder. The analysis produced three principal component vectors in three dimensions namely PC1, PC2, and PC3 which represents the orientation of the torso in 3D space. These three-dimensional vectors represent the instantaneous orientation of the torso at each frame.

PC1 represents the longitudinal orientation of the torso. Changes in this orientation (i.e., the directional change of the PC1 vector) imply the extent of torso forward bending when completing assessment activity. On the other hand, PC2 represents the extent of shoulder 'hike' and PC3 explains the torso rotation around the vertical axis.

The flexion/extension angle (α_k), axial rotation angle (γ_k) and lateral flexion angle (β_k) using Torso PCA Frame are computed using the direction cosines of the principal component vectors with the global orientation reference {$\mathbf{b_x}$, $\mathbf{b_y}$, $\mathbf{b_z}$} in the direction equal to {$\mathbf{X_G}$, $\mathbf{Y_G}$, $\mathbf{Z_G}$}. These are presented in (9) – (11).

$$\alpha_K = \cos^{-1}\left(\frac{PC1_y.b_y}{\sqrt{PC1_x^2 + PC1_y^2 + PC1_z^2}}\right) \quad (9)$$

$$\gamma_K = \cos^{-1}\left(\frac{PC3_z.b_z}{\sqrt{PC3_x^2 + PC3_y^2 + PC3_z^2}}\right) \quad (8)$$

$$\beta_K = \cos^{-1}\left(\frac{PC2_x.b_x}{\sqrt{PC2_x^2 + PC2_y^2 + PC2_z^2}}\right) \quad (9)$$

IV RESULTS AND ANALYSIS

A two-way repeated measures ANOVA was run to determine the effect of different torso orientation models on determining the torso clinical angles when performing two planar tracing tasks, circle, and point-to-point drawing. Three measures of clinical angles were assessed: lateral flexion, forward bending (forward flexion) and axial rotation. All the clinical angles were computed based on the ISB definition of clinical angles of the thorax using Grood and Suntay joint coordinate system. TPCA was compared to clinical thorax orientation for validity, and against Kinect's readily available chest orientation for superiority.

Analysis of studentized residuals showed that there was normality as assessed by Shapiro-Wilk's test of normality. There were no outliers as no studentized residuals were greater than ±3 standard deviations. Using Mauchly's test of sphericity to assess the variances of the differences between the levels of within subject's factor, the variances between the different torso models and the two planar tasks were significant at p = .018. Therefore, the Greenhouse-Geisser correction value was used instead to determine the effect size. Since the computed ε = 0.612 which was less than 0.75, the correction was necessary as suggested in previous research [12].

Data are mean ± standard deviation and reported in degrees unless otherwise stated. There was a statistically significant interaction between the different torso models and the two planar tasks assessed, F(1.225,11.022)=89.567, p<.0005, partial η^2 = .909. Therefore, simple main effects were run to determine the underlying cause of interaction.

By removing the effect of the task performed, Mauchly's Test of Sphericity yielded no significant difference in the variances between the torso models in circle tracing task, (p = 0.995, χ^2 = 0.995). Forward bending angles computed using TPCA and Kinect's chest orientation were significantly different from the computed clinical angle, F(2,18) = 126.418, p < .0005

Table- IV: Pairwise comparison between TPCA, Kinect's chest orientation and clinical model

Torso Angle	Task	Clinical-TPCA					Clinical-Kinect's Chest				
		Δμ	*Std. Error*	*Sig.*	*95% CI*		*Δμ*	*Std. Error*	*Sig.*	*95% CI*	
					Lower Bound	*Upper Bound*				*Lower Bound*	*Upper Bound*
Forward bending	CT	3.700	0.473	0.000	2.313	5.086	7.447	0.460	0.000	6.097	8.796
	PTP	0.103	0.881	1.000	-2.481	2.688	-8.341	1.393	0.001	-12.426	-4.256
Lateral Flexion	CT	1.752	0.935	0.281	-0.990	4.494	6.702	0.560	0.000	5.060	8.344
	PTP	1.631	1.456	0.875	-2.640	5.902	-1.168	0.381	0.040	-2.285	-0.051
Axial rotation	CT	-3.349	1.091	0.050	-6.55	-0.149	-5.847	3.277	0.324	-15.459	3.765
	PTP	-3.488	2.765	0.717	-11.600	4.623	0.029	1.680	1.000	-4.899	4.956

TPCA computed a significantly smaller mean forward bending angle in this task in comparison to clinical thorax model, (−3.700 ± 1.387). Forward bending angles computed using Kinect's intrinsic model were also significantly smaller than the clinical model at (−7.447 ± 1.350) also, significantly smaller than TPCA at (−3.747 ± −1.385).

Lateral flexion angles computed using TPCA and Kinect's chest orientation were significantly different from the computed clinical angle, F(2,18) = 40.072, p < .0005.

Further analysis revealed that TPCA computed a smaller mean lateral flexion angle (but not significant) in this task in comparison to clinical thorax model, (−1.752 ± 2.742), F(1.104,124.477) = 2.858, p=.12. Lateral flexion angles computed using Kinect's intrinsic model, however, were significantly smaller than the clinical model at (−6.702 ± 1.642), F(2,18) = 40.072, p<.0005.

In point-to-point (PTP) task, the variances of the difference in angles between the torso models were significant, p = .006, ε_G = 0.582. Since the epsilon computed was lower than 0.75, the Greenhouse-Geisser correction was used to determine the within-subject effect. Forward bending angles computed by the models in PTP tasks were significantly different, F(1.165,10.483) = 44.310, p < .0005. However, upon inspection, the difference between the mean forward bending angles between TPCA and the clinical model was insignificant (0.103 ± 2.585, p = 1.000). On the other hand, the difference between the forward bending angles computed using Kinect's model and the clinical model was significant (−8.341 ± 4.085, p = .001). Similarly, in CT task, the forward bending angles computed by the models were significantly different, F (2,18) = 126.418, p < .0005 and both Kinect's and TPCA were significantly different than the clinical model.

For lateral flexion angles, there was no significant difference between the torso models, F (1.104,9.939) = 2.858, p = .120 in PTP task but were significant in CT task, F (2,18) = 40 .072, p < .0005. Further inspection showed that the difference in mean lateral flexion angles between the clinical model and TPCA was insignificant at 1.752 ± 2.742, p = .281

while Kinect's model was significantly different in both tasks.

As evident in Table IV, axial rotation angles were recorded with no significant difference across models on both tasks.

V. DISCUSSION

Previous research has shown that most common impairment after stroke is hemiparesis, which is the critical indicator whether or not a patient will engage in Activities of Daily Living (ADL) when they reach a chronic stage (6 months after stroke) [13]. Abnormal synergies predominantly occurred after chronic stage from those who have an unresolved impairment. Modular organization of muscle synergies was affected which results in loss of independent joint control hence impair the movement and normal access to the workplace.

In stroke patients, pathological patterns that emerge were 'lower dimensional' than healthy individuals. It means that more co-dependencies were present between the segments of the upper limb, thus reducing the freedom of using the redundant capability of arm and forearm to perform ADL. However, other compensatory strategies such as the use of shoulder hike and torso axial rotation can still be used to complete the task, which can be observed in many patients which had poor spontaneous recovery during the sub-acute stage. Hence, assessment of movement quality after stroke was not only limited to functional activities completion but also those intrinsic to the abnormal synergies.

In current clinical assessment, these co-dependencies lie in the tasks requiring synergistic behavior of arm and forearm in gross movement, without monitoring the minute improvement in end effector quality of movements. Thus, the extent of joint inter-dependencies assessed in these tasks was still limited, as fie end effector control which is required on the daily basis such as writing was not assessed. This lack of assessment limits the inferential knowledge about patient's capability to perform tasks which require not only arm-forearm coordination but also a stable pattern of hand movements.

Previous research has presented the use of planar assessment task, typically used in a robot rehabilitation setting in which a stable pattern of hand movements can be outlined.

Movement quality is assessed through measures of temporal efficiency, movement planning, spatial accuracy, spatial efficiency, ease, smoothness and range [14]. However, in this setting, compensatory behavior mainly from the use of torso compensation to aid arm transport was not typically measured because the torso harness was used during the assessment.

While reduced arm forearm coordination can be prominent in this assessment setup, it prohibits the natural way of completing a task. That is lack of coordination which restricts the normal strategy of completing the task may be pronounced but whether a stable pattern of hand movements can be attained is unknown as compensation was restricted. The ability to measure torso movements along with end effector movement quality can be influential in a stroke research setting. It is currently known that any stroke patient will not be able to recover to his/her original motor capacity fully. Thus, the extent of impairment that maximizes the functional capability and can be outlined either from compensation or close-to-normal movement setting is desirable.

Torso movements can be defined from the change in its orientation over time. Excessive torso movement such as shoulder hike and forward bending to reach objects in space can be outlined by higher lateral flexion angle and forward bending angle in comparison to normal movement. By computing the differences of the measurements of TPCA in comparison to the clinical model, it can be ascertained that TPCA correctly reflected the clinical measurements if differences between the measurements were not significant.

Within this database, TPCA produced results with no significant difference to the clinical measures in lateral flexion angle and axial rotation angle in both tasks. These were not the case for Kinect's intrinsic model. These results ascertained that TPCA was superior in producing measurements that were close to the clinically accepted thorax model when measuring lateral flexion and axial rotation in performing both tasks.

On the other hand, the overall analysis showed that TPCA produced a significantly smaller forward bending angle than the clinical result. However, upon inspection, the results had no significant difference to clinical results in PTP task while

Kinect's intrinsic model was significantly different to clinical results in both tasks. Thus, the use of forward bending measurement using TPCA in PTP task would yield a similar result in comparison to clinically accepted measurements and superior to Kinect's intrinsic model.

From the task point of view, TPCA computed significantly greater means in the forward bending angle in circle tracing than PTP task similar to the clinical model. Kinect's intrinsic model however computed significantly smaller forward bending in circle tracing than PTP. These results confirmed that TPCA was able to portray similar task related outcomes with clinical model.

Unfortunately, this study was limited to torso movements when performing planar tasks, which might not extrapolate to more complex motions in ADL tasks. However, reaching from contralesional space to ipsilesional space which was intrinsic to both tasks was desirable to outline temporal efficiency in stroke patients [15], [16]. With the additional information on torso movements, the temporal efficiency can be discerned to the extent of compensatory strategies used to attain them.

V. CONCLUSION

Forward bending, lateral flexion and axial rotation angles computed with TPCA when performing point-to-point task were not statistically significantly different to the angles computed with the clinical model. Kinect's intrinsic chest orientation angles were however statistically significantly different than the clinical model.

Thus, the TPCA model is concurrently valid with the clinically accepted measures of torso orientation and can be used further to analyze torso compensation in stroke patients.

VI ACKNOWLEDGMENT

This work was performed under financial support from the University of Auckland, New Zealand and the financial support from Universiti Teknikal Malaysia Melaka through short term grant, PJP/2018/FKE(7D).

REFERENCES

1. S. Michaelsen, A. Luta, A. Roby-Brami and M. Levin, "Effect of trunk restraint on the recovery of reaching movements in hemiparetic patients," Stroke, 32(8), 2001, pp. 1875-1883.
2. S. Brunnstroem, Movement Therapy in Hemiplegia-A Neurophysiological Approach. New York: Harper and Row, 1970.
3. M. Levin, J. Kelim, and S. Wolf, "What do motor "recovery" and "compensation" mean in patients following stroke?," Neurorehabilitation and Neural Repair, 23(4), 2009, pp. 313-319.
4. M. Levin, S. Michaelsen, C. Cirstea, and A. Roby-Brami, "Use of the trunk for reaching targets placed within and beyond the reach in adult hemiparesis," Experimental Brain Research, 143(2), 2002, pp. 171-180.
5. C. Y. Wu, C. L. Yang, M. D. Chen, K. C. Lin, and L. L. Wu, "Unilateral versus bilateral robot-assisted rehabilitation on arm-trunk control and functions post stroke: A randomized controlled trial," J. Neuroeng. Rehabil., 10, 2013, pp. 1-10.
6. N. Nordin, S. Q. Xie, and B. Wünsche, "Simple torso model for upper limb compensatory assessment after stroke," IEEE International Conference on Advanced Intelligent Mechatronics, pp. 775-780, 2016.
7. J. M. Wagner, C. E. Lang, S. A. Sahrmann, D. F. Edwards, and A. W. Dromerick, "Sensorimotor impairments and reaching performance in subjects with poststroke hemiparesis during the fist few months of recovery," Phys. Ther., 87(6), 2007, pp.751–765.
8. A. De Los Reyes-Guzmán, I. Dimbwadyo-Terrer, F. Trincado-Alonso, F. MonasterioHuelin, D. Torricelli, and A. Gil-Agudo, "Quantitative assessment based on kinematic measures of functional impairments during upper extremity movements: A review," Clin. Biomech., 29(7), 2014, pp. 719–727.
9. T. A. Jones, "Motor compensation and its effects on neural reorganization after stroke," Nat. Rev. Neurosci., 18(5), 2017, pp. 267–280.
10. G. Wu, F. C. T. Van Der Helm, H. E. J. Veeger, M. Makhsous, P. Van Roy, C. Anglin, J. Nagels, A. R. Karduna, K. McQuade, X. Wang, F. W. Werner, and B. Buchholz, "ISB recommendation on defiitions of joint coordinate systems of various joints for the reporting of human joint motion - Part II: Shoulder, elbow, wrist and hand," J. Biomech., 38(5), 2005, pp. 981–992.
11. J. Brekelmans. (2014). Kinect Brekel Probody v2. [Online]. Available: http://brekel.com/brekel-pro-body-v2/.

AUTHORS PROFILE

Nurdiana Nordin is a lecturer at the Faculty of Electrical Engineering, Universiti Teknikal Malaysia Melaka. She earns B.Eng (Mechatronics) from IIUM, M.Sc (Mechatronics) from University of Siegen and PhD (Mechatronics) from University of Auckland. Her research is mainly focused on the application of computer vision as an aid for stroke assessment in the vision of automating rehabilitation assessment in the future.

Prof. Sheng-Quan Xie is currently the Chair in Robotics and Autonomous Systems (2017-) in the University of Leeds. e received his BE in Control Engineering, M.Sc., and Ph.D. in Mechatronics Engineering from Huazhong University of Science and Technology (HUST), China, in 1992, 1995, and 1998, respectively. He was a Research Associate (1998-1999) and a FoRST (Foundation for Research, Science and Technology) Postdoctoral Fellow (1999-2002) at the University of Canterbury and was awarded a second PhD in Mechanical Engineering. He worked in the University of Auckland, New Zealand as Lecturer (2003-2005), Senior Lecturer (2006-2009), Associate Professor (2010-2011) and Chair Professor (2011-2017), in Mechatronics Engineering. Prof Xie's research is in the areas of advanced mechatronics and robotics in medicine and high value industries. His principal research interest is in the development of new robotic technologies for a wide range of applications ranging from rehabilitation, medical surgery, and personal assistance to industrial applications. His research approach is to use a combination of mathematical modelling techniques, mechatronic methods, and experimental measurements to better understand human systems, design smart and robust robotic devices and automatically control them interacting with human.

Burkhard Wünsche is a Senior lecturer in the School of Computer Science, Faculty of Science, University of Auckland. He is the Director of the Division for Biomedical Imaging and Visualization. His research interests include Scientific and Biomedical Visualization, Medical Imaging, Information Visualization, Computer Graphics, Game Technology, Computer Aided Geometric Design, Simulation Algorithms, Virtual Reality (VR) and Augmented Reality (AR), Human Computer Interfaces (HCI), Computer Vision, and Cognitive Psychology. He has collaborated with various research centers and industries in pursuit of his research notably Royal New Zealand Navy (RNZN) - Defense Technology Agency (DTA), Auckland, New Zealand, AIST, National Institute of Advanced Industrial Science and Technology, Tokyo, Japan, Visualization Center C, Norrköping, Sweden and ETRI (Electronics and Telecommunications Research Institute), Daejeon, South Korea.